33RD CONGRESS
OF THE INTERNATIONAL COUNCIL
OF THE AERONAUTICAL SCIENCES
STOCKHOLM, SWEDEN, 4-9 SEPTEMBER, 2022

ICAS 2022 SWEDEN

DAMAGE QUANTIFICATION ON COMPOSITE STRUCTURES USING NEURAL NETWORKS AND HYBRID DATA

Leonardo de Paula Silva Ferreira[1*], Marcos Omori Yano[2], Samuel da Silva[3] & Carlos Alberto Cimini Júnior[4]

[1]UFMG - Universidade Federal de Minas Gerais, Brasil
[2]UNESP - Universidade Estadual Paulista, Campus de Ilha Solteira, Brasil
[3]UNESP - Universidade Estadual Paulista, Campus de Ilha Solteira, Brasil
[4]UFMG - Universidade Federal de Minas Gerais, Brasil

Abstract

In the aeronautic industry, in addition to the aging of the current fleet of aircraft in operation, increasing cargo capacity and the use of composite materials have increased interest in developing Structural Health Monitoring systems (SHM) by aircraft manufacturers and airlines. On the other hand, the increase in the processing capacity of computers enabled the development of Artificial Intelligence systems. These systems can make decisions based on an incomplete data set and are particularly attractive in applications where human intelligence and critical thinking are needed. However, the performance of SHM based on Machine Learning is limited to only the knowledge used in the learning phase, not able to describe the structural behavior under conditions different from those used in the model training. This work proposes a hybrid learning methodology as an alternative to augment the amount of data available during the training phase. A finite element model is adjusted with limited experimental data and used to simulate new damage scenarios. Then, a multilayer neural network is trained with different experimental and numerical data combinations. The system's performance is evaluated with experimental data that is not used during model training, and the model's accuracy is compared using scenarios with and without

Keywords: SHM, neural networks, Lamb wave simulations, hybrid learning

1. Introduction

The main objective of Structural Health Monitoring (SHM) systems is to identify changes at the earliest possible opportunity so that corrective action can be scheduled and minimize downtime, operating and maintenance costs, and reduce the risk of catastrophic failures during operation. Massive adoption of SHM systems in aerospace structures can improve safety and reliability while reducing downtime and associated costs. With the aging of the fleet of aircraft in operation, maintenance costs increase and can reach up to a quarter of the fleet's operating cost [1].

According to Mitra and Gopalakrishnan [2], one of the main techniques for use in SHM is those based on guided waves. Among the various forms of guided waves, Lamb waves are the most applied to thin structures [3]. For use in SHM, Lamb waves can be generated and captured in the system through piezoelectric sensors of the PZT type. These sensors deform when subjected to electrical voltage and induce an acoustic vibration in the structure. This vibration propagates and can be measured by other sensors scattered in it. By measuring the behavior of Lamb waves in an undamaged structure, a Baseline signal can be obtained. Subsequent measurements are compared to the baseline, and detection techniques can be used to locate and quantify the damage.

Damage detection from the measured signals can be performed in different ways. Among the detection techniques presented in the literature, we can highlight those based on the transformation between time and frequency domains, such as the Wavelet transform used by Chen et al. [4], the Short Term Fourier Transform (STFT) used by Liu et al. [5], and the Hilbert and Hilbert-Huang transform, used by Wang et al. [6].

There are also machine learning (ML) techniques, which are particularly efficient in cases in which the phenomena studied have complex characteristics and non-linear behavior. These techniques use data collected from previous cases, which are used to generate a classification model based on the input data. Among the methods based on ML, Mitra and Gopalakrishnan [2] highlight the Artificial Neural Networks (ANN), which are algorithms inspired by biological structures that mimic the behavior of the nervous system of living beings. These algorithms are organized into different architectures, from the simplest to the most complex, such as multilayer networks (MLP), Convolutional Neural Networks (CNN), Evolutionary Neural Networks, Adaptive Neural Networks, etc.

Models based on machine learning have gained increasing relevance and application in the field of structural monitoring due, among other factors, to the ability of algorithms to adapt to different applications and flexibility regarding the architectures available for use. Therefore, the use of neural networks for detecting damage in aerospace structures is a promising field of research, both for the adaptability of artificial intelligence models and the increasing amount of data available for analysis.

One of the main limitations of Machine Learning based systems is the amount of data needed to train the classification models. The production of part of this data using numerical simulations have the potential to reduce the number of tests needed to obtain training data. The system can also be simulated in damage scenarios that cannot or are too expensive to test. It can also accelerate the development of damage detection systems. This work aims to develop a damage classifications model based on neural networks that can be trained with a dataset of numerical and experimental data and compare its results with different data combinations.

2. Literature review

2.1 Structural Health Monitoring

Structural Health Monitoring (SHM) is an area that combines an instrumented structure and a system with algorithms that ask the structure for its “health” or condition in real-time or as needed [7].Giurgiutiu [8] states that an SHM system can be passive or active. A passive approach is based on measuring operational factors and obtaining the state of the structure based on them. For example, in an aircraft, one can monitor parameters such as speed, vibration levels, turbulence levels, etc., and use algorithms to determine the state of the structure. On the other hand, active systems use sensors scattered throughout the structure to detect the damage's presence and extent. An active SHM system has similar premises to non-destructive testing (NDE) systems. Still, with an extra level: SHM systems aim to install permanent sensors in the structure for analysis whenever necessary.

The development of piezoelectric sensors based on Lead Zirconate Titanate (PZT) made it possible to reduce the cost of instrumentation needed for SHM systems compared to traditional NDE sensors [8]. These versatile sensors are manufactured in different formats and affixed to the structures or included during manufacturing. Damage detection with piezoelectric sensors can be performed in a few ways: guided wave propagation, frequency response function, or electromechanical impedance.

According to Giurgiutiu [8], guided waves are ultrasonic mechanical waves propagating through structures, remaining within the walls of thin-walled structures, and traveling great distances. These properties allow its application in the ultrasonic inspection of aircraft, missiles, pressure vessels, storage tanks, etc. Lamb waves, also known as guided plate waves, are a type of guided wave that propagates between two free parallel surfaces of a thin-walled structure.

For use in SHM, Lamb waves can be generated and captured in the structure through piezoelectric sensors of the PZT type. These sensors deform when subjected to electrical tension and induce an acoustic vibration in the system. This vibration propagates and can be measured by other sensors scattered in it. By measuring the behavior of Lamb waves in an undamaged structure, a “signature” (also called Baseline) can be obtained. Subsequent measurements are compared to the signature, and detection techniques can be used to locate and quantify the damage. Among these techniques, we have those based on neural networks.

2.2 Neural Networks

Artificial intelligence emerged as a branch of computer science in the 1950s. Since then, it has produced tools that can be applied in engineering to solve problems where human intelligence is needed [9]. Among the available algorithms, artificial neural networks (ANN) have stood out due to their non-linearly capability and ability to generalize and extrapolate knowledge based on an incomplete data set. A neural network is a computational model of the brain. Models based on neural networks are built from basic units called neurons, which are interconnected and perform calculations in parallel.

A neural network learns based on a process called training, which can be supervised or unsupervised. In supervised training, the neural network is presented with input data and the expected response. Based on the data provided, the network adapts and adjusts its parameters, storing the learning in the weights of connections between neurons. In unsupervised training, the neural network is presented with input data only and learns by grouping the data into classes with common characteristics. After training, the neural network is submitted to a set of data it has never had contact with, and its efficiency is measured based on the success rate with this data.

Neural networks can also be classified by type. Among the most common types, there are the Multilayer Perceptron (MLP) neural networks. According to Pham [9], this type of neural network is more common due to its ease of implementation and robustness. It consists of a series of interconnected neurons, creating layers. The inputs of each neuron are weighted and summed to a constant value, called bias. The neuron then applies the sum value to a transfer function and outputs the result, as shown in Eq. 1 [10].

$$x(k) = T\left(\sum_{i=0}^{m} w_i(k)y_i(k) + b\right) \tag{1}$$

In which:
$y_i(k)$ is the value of the discrete-time input k,
$w_i(k)$ is the value of the weight in discrete time k
b is the bias
T is the transfer function (also called activation function)
$x(k)$ is the value of the neuron output

2.3 Damage indices

The input data to a neural network is essential for the quality of the analysis. In SHM applications, this data is treated in the form of indices indicating the structure's state, commonly called damage indices (DIs). For each data set, damage indices can be calculated in several ways, including those proposed by Dworakowski et al. [11]. Among the indices presented by the author, there is the RMS error of the signal, the cross-correlation, and the difference between the Hilbert transform and the Fourier transform. Combined, these damage indices can assess attenuations and delays in the responses of Lamb waves both in the time domain and frequency domain. The damage indices can then be used as input information for a model based on neural networks. Four damage indices proposed by Dworakowski et al. [11] and shown in Tab. 1 were used in the present work.

Table 1 – Damage indices used as ANN's input

	Index name	Equation	Comments
1	DI_{TDRMS}	$DI_{TDRMS} = 1 - \frac{\int_{t1}^{t2}[y(t) - x(t)]^2 dt}{\int_{t1}^{t2} x(t)^2 dt}$	Identify attenuation in damaged signal.
2	DI_{XCOR}	$DI_{XCOR} = 1 - r_{xy}(\tau = 0)$	Identify differences of phase and shape between signals
3	$DI_{maxXCOR}$	$DI_{maxXCOR} = 1 - max\left(r_{xy}(\tau)\right)$	Identify differences of phase and shape between signals
4	DI_{ENV}	$DI_{ENV} = 1 - \frac{\int_{t1}^{t2}[Y(t) - X(t)]^2 dt}{\int_{t1}^{t2} X(t)^2 dt}$	Identify changes in amplitude and frequency between signals.

In Tab. 1, $y(t)$ e $x(t)$ are the signs of the structure with and without damage, respectively, and t_1 and t_2 are the integration intervals. $X(t)$ and $Y(t)$ represent the signature envelopes, for instance the Fourier Envelope and $r_{xy}(\tau)$ represents the cross-correlation operation. According to [11], the advantage of correlation indices is that if the signal with damage and without damage are identical, the cross-correlation becomes the autocorrelation and has a maximum value of 1 at $\tau = 0$. This means that this indicator is only sensitive to changes in signal shape and phase, not changes in amplitude.

3. Methodology

3.1 Experimental setup

A CFRP plate with dimensions of 500 x 500 x 2 mm^3 is used in this article. It comprises 10 layers of carbon fibers unidirectionally aligned along a 90° direction and stacked in an epoxy resin matrix. The composite plate is instrumented with four PZT transducers SMART Layer manufactured by Acellent Technologies Inc. The structure is excited by a five-cycle sinusoidal tone burst, and center frequency of 250 kHz applied on PZT 1. Then PZT 2 is used as a sensor to acquire the output signal. Fig. 1 presents a schematic overview of the experimental setup used.

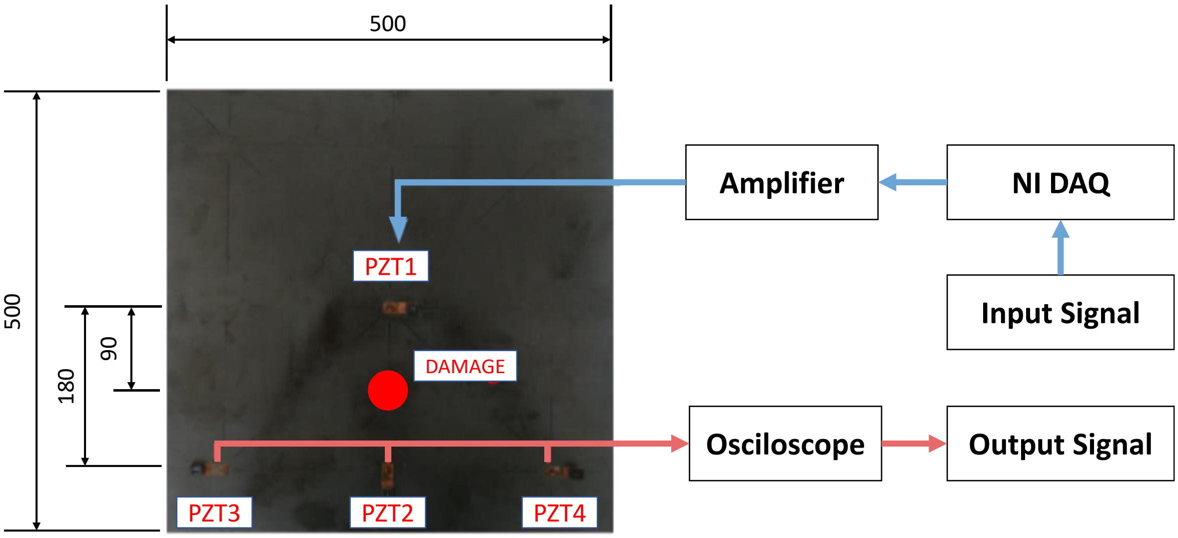

Figure 1 - Composite plate and schematic view of the experimental setup (measurements in mm). Adapted from [12]

Damage is simulated by inserting an adhesive putty on the surface's plate. This additional localized mass simulates local changes in the damping of the plate, which has some similarities to delamination in composites structures, as reported by Lee et al. [13]. This is a common practice in the literature to simulate damage reversibly, i.e., without damaging the structure. Tab. 2 shows the damage nomenclature and the amount of mass added to each, and Fig. 2 compares baseline and damaged signals.

Table 2 – Damage conditions used in the experimental setup

	$H^{\{t\}}$	$D_1^{\{t\}}$	$D_2^{\{t\}}$	$D_3^{\{t\}}$	$D_4^{\{t\}}$	$D_5^{\{t\}}$	$D_6^{\{t\}}$	$D_7^{\{t\}}$	$D_8^{\{t\}}$	$D_9^{\{t\}}$	$D_{10}^{\{t\}}$	$D_{11}^{\{t\}}$
Covered area [%]	0	0.196	0.282	0.384	0.502	0.785	0.950	1.13	1.53	2.01	2.27	2.54

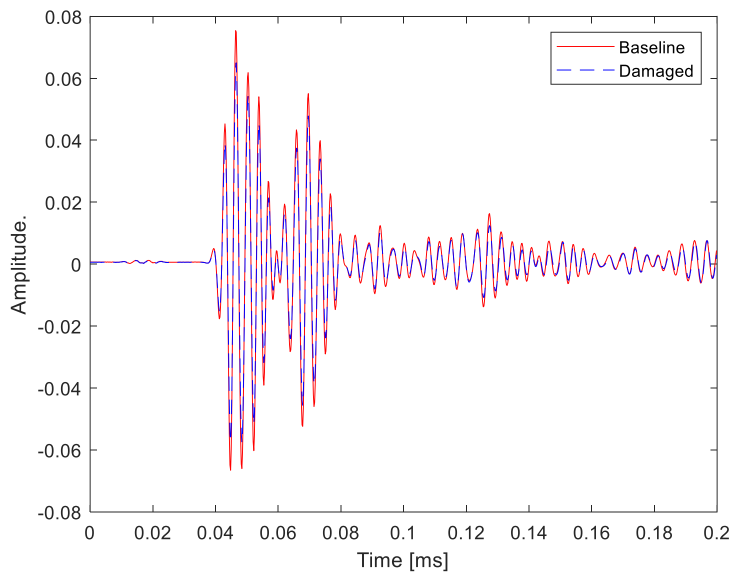

Figure 2 – Comparison between the signal from healthy and damaged conditions

3.2 Numerical model

To replicate the experimental setup, a finite element model has been implemented in Abaqus 6-14. The plate has been modeled as a solid structure and meshed with continuum shell elements (SC8R). The piezoelectric actuator and sensor were implemented as circular cells. As a strategy to allow the creation of a mapped mesh, the PZTs were bounded with a square region, as shown in Fig. 3 (a)(c). The same amplitude used in the experiment was applied as a planar radial force at the PZT borders, as shown in Fig. 3 (b). As boundary conditions, plate borders were maintained free.

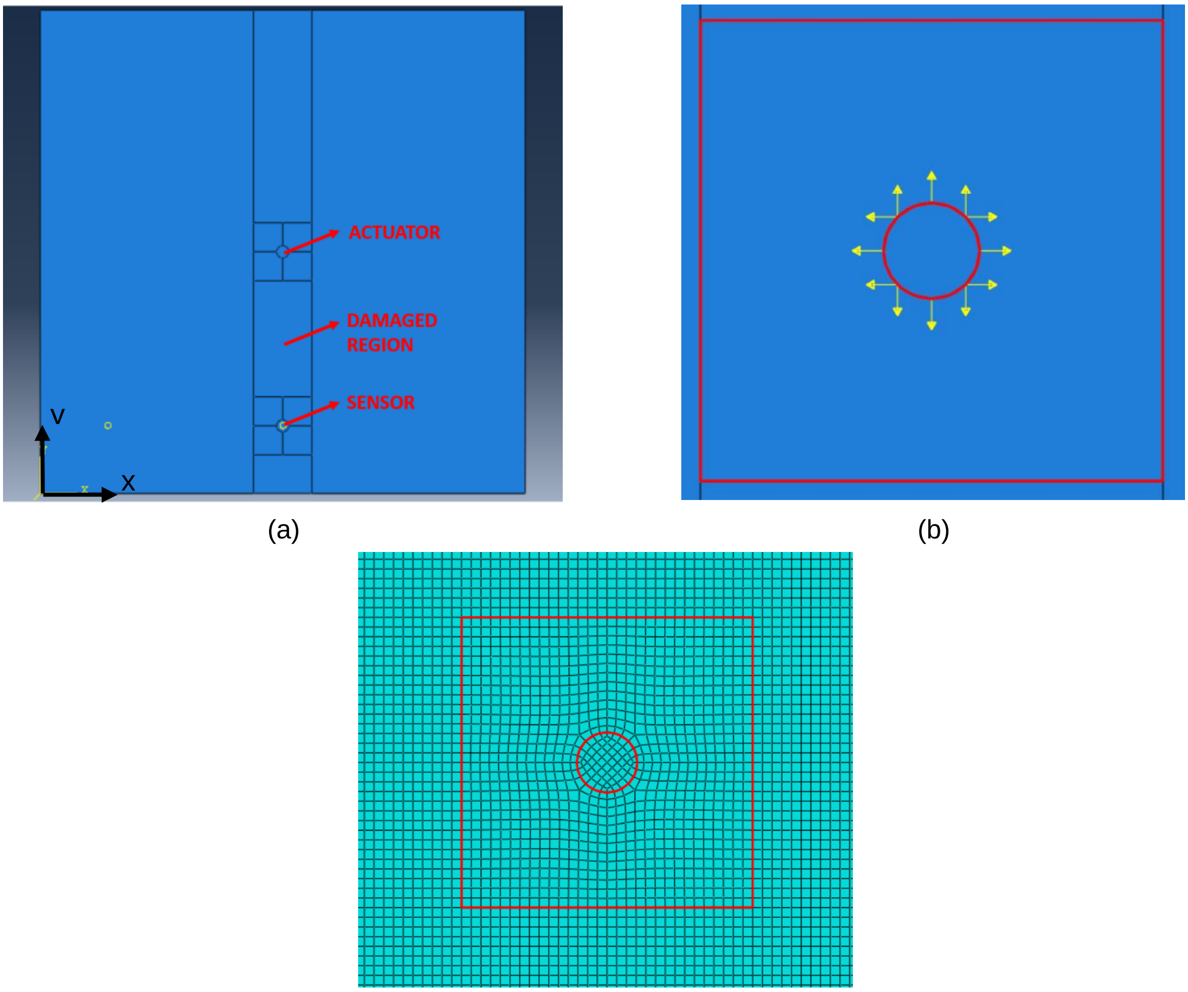

Figure 3 – FE model showing (a) axis orientation, actuator, sensor, and damaged region, (b) applied loads, and (c) mesh around the PZT

The stacking sequence of the laminate is unidirectional with $[90_{10}]$ layup orientation with respect to the X axis in Fig. 3. Each layer is composed of an elastic material with engineering constants shown in Tab. 3, implemented as a laminate property.

Table 3 - CFRP properties

E_1 [MPa]	E_2 [MPa]	E_3 [MPa]	ν_{12} [ ]	ν_{13} [ ]	ν_{12} [ ]	G_{12} [MPa]	G_{13} [MPa]	G_{23} [MPa]	$\rho\ \left[\frac{kg}{m^3}\right]$
147	10.3	10.3	0.27	0.27	0.54	7.0	7.0	3.7	1600

An Explicit analysis has been developed. Lamb wave propagation is a dynamic non-linear problem, and convergence and stability results depend on the correct mesh sizing and time step. According to Gresil et al. [14], 20 elements per wavelength are needed for a good spatial resolution. This condition resulted in an average element size of 2 mm. Also, according to Gresil et al. [14], the maximum stable time step can be estimated as shown in Eq. (2), resulting in 0.2 μs. Further testing showed that a time step of 0.1 μs produced stable results with a reasonable simulation time. Abaqus2Matlab routine [15] was used to integrate MATLAB with Abaqus and simulate several conditions in sequence.

$$\Delta t = \frac{1}{20 f_{max}} \tag{2}$$

3.3 Neural Network architecture

The neural network models were implemented using the MATLAB Deep Learning toolbox. A multilayer neural network with one hidden layer was used. In the input layer, four neurons were used, one for each damage index shown in Tab. 1. Damage indices were calculated as presented in section 2.4, using the damaged signal and the baseline. Twenty neurons were used in the hidden layer and one neuron in the output layer, responsible for indicating the severity of the damage. As an activation function, the ReLU function was used. The model was trained using the Root Mean Square Propagation (RMSprop) optimization algorithm. The learning rate started at 0.001 and decreased every certain number of epochs to minimize overfitting.

The model was trained in three different scenarios, as shown in Fig. 4. These conditions portray real procedures in which training can be performed: (1) with only limited experimental data, (2) using only numerical data generated by a model, and (3) using limited experimental data together with numerical data to extend the training spectrum. All scenarios were evaluated using the same test data. The test data aims to assess the model's ability to generalize under conditions with which it had no contact during the training stage.

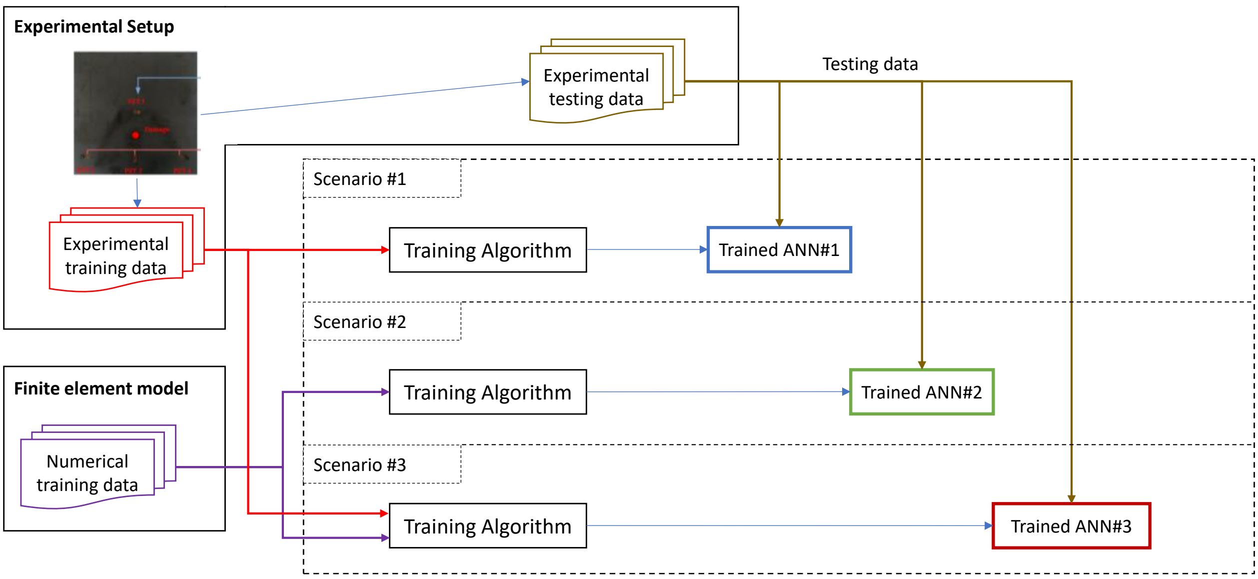

Figure 4 – Training and testing layout

Tab. 4 presents the damage conditions used in each scenario. Labels D_1 to D_{11} refer to damaged areas in Tab. 2.

Table 4 – Datasets used in training and learning phase

Scenario	Data used in training phase	Data used in the testing phase
(1) Experimental data only	EXP: [D_1, D_3, D_4, D_6, D_9, D_{11}] FEM: [ ]	[D_2, D_5, D_7, D_8, D_{10}]
(2) Numerical data only	EXP: [ ] FEM: 12 conditions	
(3) Hybrid training - Experimental and numerical data	EXP: [D_1, D_3, D_4, D_6, D_9, D_{11}] FEM: 12 conditions	

Model's performances were evaluated by comparing the root mean square error (RMSE) between the neural network prediction for a given condition and the experimental results. In addition, the training process of each condition and possible convergence problems in the optimization algorithm for training were evaluated.

4. Results and discussions

4.1 Finite element model adjustment

Fine-tuning of the model was performed to approximate the numerical results obtained through the finite element model from the experimental ones. The adjustment was made by modifying the mechanical properties of the composite material to get similar response curves. The model was initially adjusted for the healthy condition. At this stage, the mechanical properties were modified to adjust the Lamb wave's propagation time and shape. Fig. 5 compares the experimental data for the healthy plate and the simulated model results.

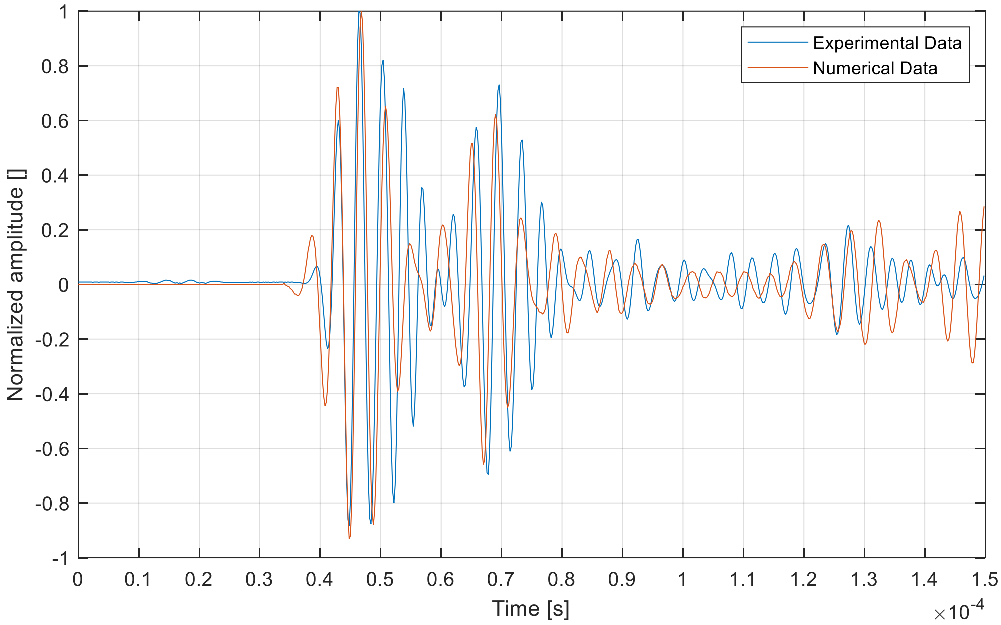

Figure 5 – Comparison between experimental and numerical data in healthy conditions

The addition of damage in the numerical model was done by modifying the properties of the last layers of the laminate to simulate the change in the local impedance of the structure caused by delamination. Numerically, the damage severity can be simulated by modifying the number of layers with altered properties, the stiffness and mass properties of the composite material, and the extent of the damaged area, all of which modify the plate impedance and alter the propagation of Lamb waves. The model was created to iteratively simulate multiple damage conditions, and enable the automation of tests in various scenarios. Modifications to the size of the damaged region require adjustments in size and shape control of local mesh, and these modifications are specific to each damage size. This is because explicit wave propagation simulations are very sensitive to the number of elements per wavelength [14] and elements distortion. This way , the damaged area was kept at a constant size to avoid the need for mesh adaptations for each simulated damage condition.

The real damage, experimentally simulated as a local mass increment, had to be correlated with the numerical results. Fig. 6 presents the experimental results for the conditions tested. The ratio between damaged and baseline peak amplitudes is shown as function area covered. There is a direct correlation between damaged area and peak amplitude reduction.

Modifying mechanical properties at the numerical model also causes changes in peak amplitude. Therefore, the peak amplitude in both cases was used as a comparison parameter between the experimental and simulated data. The same experimental training conditions shown in Table 4 were used during the adjustment of the finite element model. The finite element model was not adjusted to the conditions used for testing the neural networks, only for the training ones. Fig. 6 shows the training conditions as red dots and the testing conditions as blue dots.

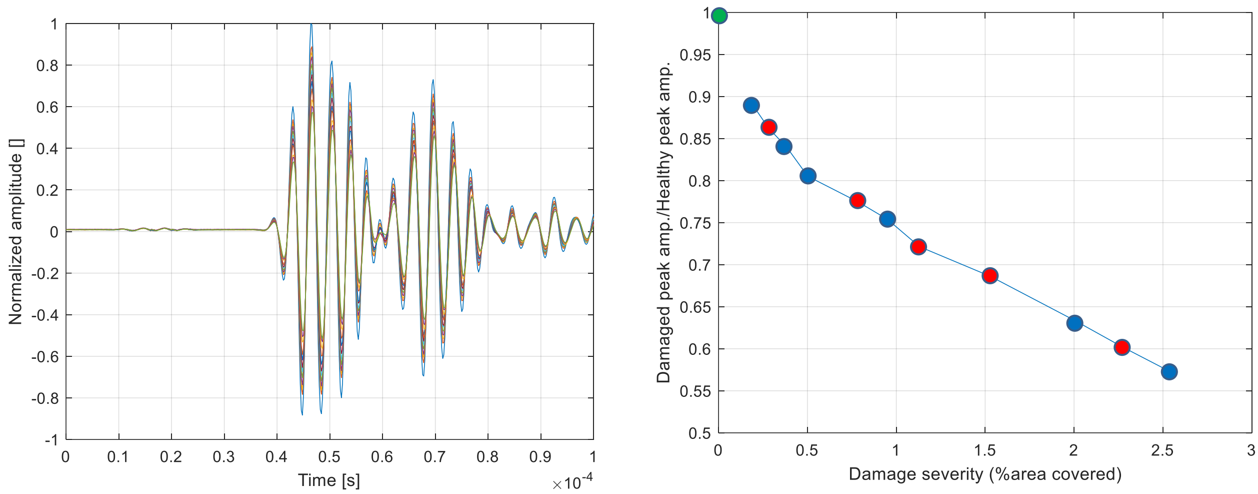

(a) (b)

Figure 6 – Experimental data (a) Dispersion curves, (b) damage impact on peak amplitude. Baseline (●), Training data (●) and Test data (●)

Fig.7 shows the dispersion curves for experimental and numerical datasets.

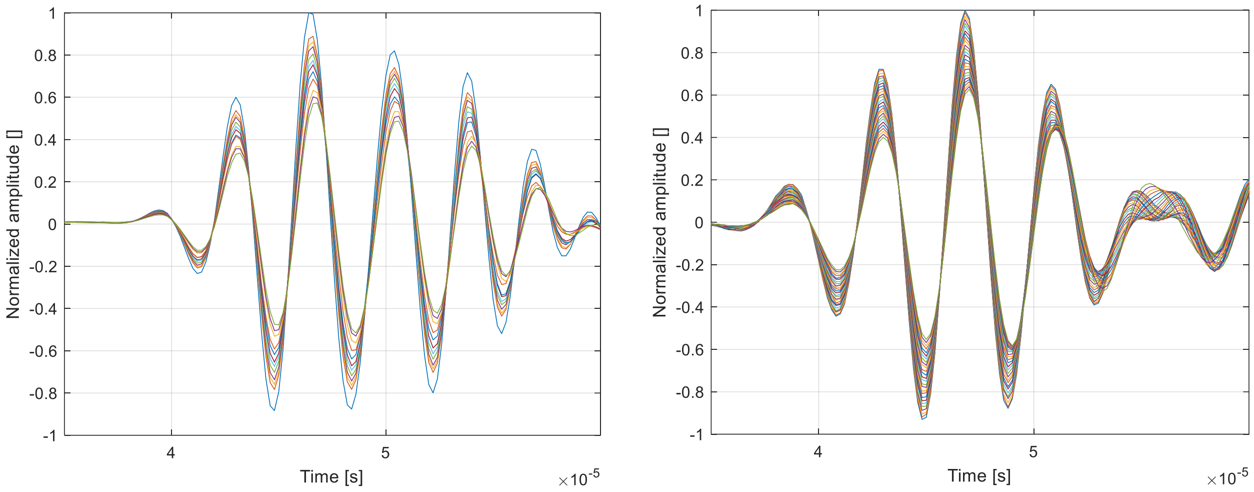

(a) (b)

Figure 7 – Dispersion curves (a) Experimental dataset, (b) Numerical dataset

The similarity between the numerical model and the actual structure can also be evaluated by comparing the damage indices in Fig. 8. This figure shows the damage indices of difference between the root mean square value of the signal in the time domain (TDRMS), the difference between the signals in the frequency domain (FOURIER), the correlation between the signals with zero delay (XCOR) and maximum correlation between the signals ($XCOR_{max}$). The behavior of the numerical model is similar to the experimental data when comparing the TDRMS and FOURIER indicators. This is because the model adjustment was performed based on the peak value of the output signal. Also, as there are no frequency modifications with damage insertion, DI_{TDRMS} and $DI_{FOURIER}$ present similar trends. Despite this, the correlation-based DIs still manages to capture the trend of the damage index, as can be seen from the shape of the XCOR and $XCOR_{MAX}$ curves in Fig. 8. The correlation differences observed between the model and experimental data can be attributed mainly to the region after $5x10^{-5}$ s in Fig. 7. In the future, the model adjustment strategy can be modified to quantify not only differences between the peak value but also multiple wave peaks and delays in the signal.

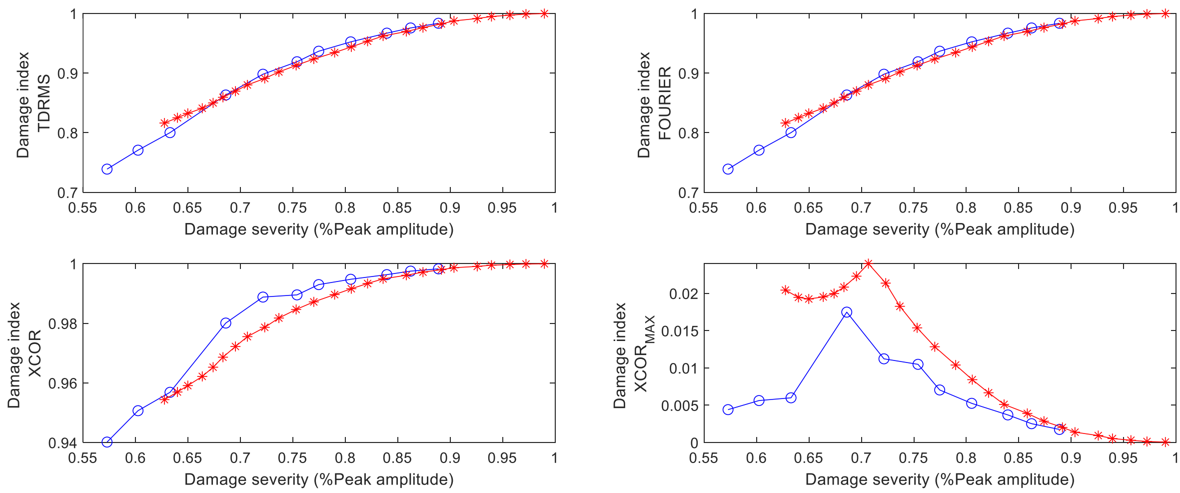

Figure 8 – Comparison between Dis obtained from experimental (o- blue) and numerical (*- red) data.

4.2 Damage quantification

One hundred neural networks were trained for each condition presented in Tab. 3. The performance of the networks was evaluated by comparing the predictions for damage severity in the five conditions not used during the training process. Fig. 9 presents the dispersion of predictions from neural networks for the three proposed training scenarios. The RMSE between the predicted and actual damage severity was calculated and used as a performance measure.

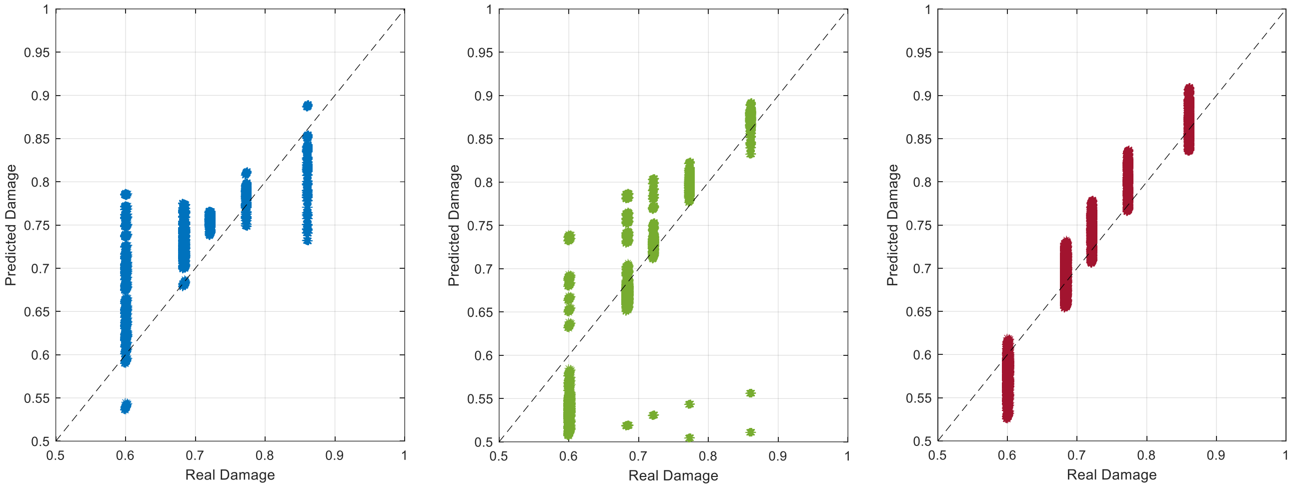

(a) (b) (c)

Figure 9 - Comparison between predicted and real damage from: (a) condition 1 – Experimental data only, (b) condition 2 – Numerical data only, and (c) condition 3 – Experimental and numerical data

The model trained with only experimental data presented more dispersion in the predictions compared to the other two scenarios. In addition, this model presented difficulty in converging in the training stage. This is due to the limited amount of information the neural network has in these cases. Training with only six damage conditions can cause the optimization algorithm to get stuck in a local minimum and be unable to obtain a satisfactory fit to the data. Fig. 10 shows examples of convergence problems during the training phase.

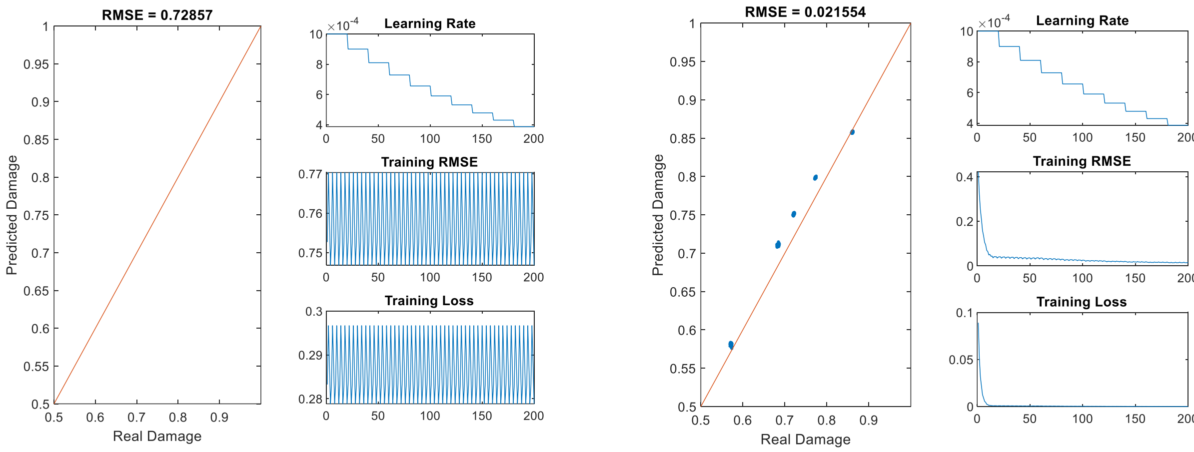

(a) (b)

Figure 10 – Convergence analysis (a) Case with convergence problems, (b)Case with convergence

Fig. 7 presents the probability dispersion for the RSME of neural network predictions. For training cases exclusively with experimental or numerical data, it is possible to observe situations in which the RMSE was greater than 0.7. These points correspond to cases where the model failed to converge to a satisfactory solution. The model based on only experimental data could not converge 50% of the time, compared to 34% of the time for the purely numerical model. The model trained with mixed data converged in all training rounds. As the strictly experimental model has little information to construct an approximation function, it has often been found in situations where the training algorithm does not converge. Even if numerically simulated, the increased amount of data fills information gaps that the model cannot perform.

Eliminating non-convergence cases, it is possible to compare the performance of networks that were able to fit the data. Tab. 5 presents the RMSE data for all cases and for only the cases that converged, in addition to the number of cases that did not. The case with hybrid training presented the best performance, with RMSE 46.7% lower than the model trained only with experimental data.

Table 5 – RMSE and convergence information

Condition	RMSE All data	# non-convergences	RMSE Converged cases only
#1 – Experimental only	0,3974	50	0,0473
#2 – Numerical only	0,2831	34	0,0303
#3 – Experimental and numerical	0,0251	0	0,0251

Fig. 11 shows the probability distribution of the RMSE, excluding cases of non-convergence in training. The model trained with hybrid data showed the lowest dispersion in the predictions and the lowest average in the RMSE. On the other hand, the models trained with only experimental data presented greater dispersion of results, performing worse than the other two scenarios.

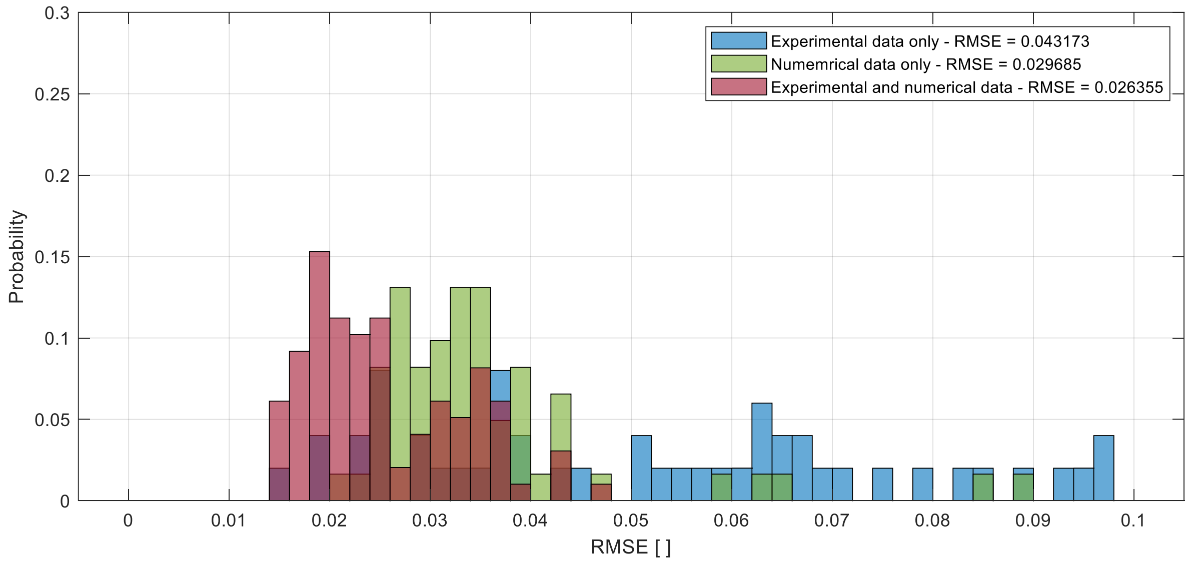

Figure 11 – RMSE probability distribution excluding non-convergence cases

Thus, the training strategy that uses mixed data presented the best performance among the three approaches. Neural networks need a large amount of data under different conditions to make predictions. Therefore, training with a limited number of conditions, as tested in the scenario of only experimental data, performs worse than the others. In a real structure, obtaining more data for training would require more tests with different damage conditions. This means more lab hours and costs involved in system development. For the plate used in this work, a well-fitted numerical model based on a limited amount of experimental data was able to simulate untested conditions and feed the neural network used as a classifier.

The predictions of the neural networks can be improved by increasing the quality of the model and adjusting the architecture of the networks as a function of the amount of data used for training. The numerical model can be improved by modifying the tuning parameters to include multi-peak amplitude effects and delays in the signal. And the network architecture can be fine-tuned based on the amount of training data, modifying the quantity of neurons and number of layers, for instance. In the present work those parameters were maintained fixed as a simplification to minimize the number of variables involved in the study.

5. Conclusions

The work presented an analysis of damage quantification in a composite material plate using multilayer neural networks and hybrid training. The analyzes were performed in three scenarios: (1) using only experimental data, (2) only simulated data, and (3) combined experimental and numerical data for training the networks. The simulated data were obtained from a finite element model fitted using healthy and damaged data. This model was then used to simulate other conditions and train the neural networks.

Neural networks were compared based on performance during the training stage and their ability to predict unknown scenarios. Models trained with hybrid data showed the best results compared to models trained only with experimental or numerical data. The mean squared error of models trained with hybrid data was 46.7% lower than models trained with experimental data only. In addition, these models showed less dispersion in damage prediction and did not have convergence problems. This approach could be used in the future with more complex structures to reduce the number of experimental scenarios needed to train a classifier in an SHM system.

6. Acknowledgements

This work has been supported by the following Brazilian research agencies: Fundação de Amparo à Pesquisa do Estado de Minas Gerais (Fapemig) and Conselho Nacional de Desenvolvimento Científico e Tecnológico (CNPq). The authors would also like to acknowledge the support of the São Paulo Research Foundation (FAPESP) grant number (19/19684-3), Coordenação de Aperfeiçoamento de Pessoal de Nível Superior (CAPES) – Brasil – Finance Code 001 and the Portuguese National Funding Agency for Science Research and Technology (FCT/Portugal) process 88881.467597/2019-01.

7. Contact Author Email Address

mailto: leonardopsf@ufmg.br

8. Copyright Statement

References

[1] Boller C, Staszewski W J, Tomlinson G, Health Monitoring of Aerospace Structures (Hoboken, NJ: Wiley). 2004.

[2] Mitra, M., Gopalakrishnan, S., Guided wave based structural health monitoring: A review, Smart Materials and Structures, vol 25, 2016.

[3] Lamb H, 1917. On waves in an elastic plate. Proceedings of the Royal Society of London.

[4] Chen X, Li X, Wang S, Yang Z, Chen B and He Z, Composite damage detection based on redundant secondgeneration wavelet transform and fractal dimension tomography algorithm of Lamb wave, IEEE Transactions on Instrumentation and Measurement 62 1354–63, 2013.

[5] Liu, G., Xi, Z., Lam, K. Y., Shang H., Detection and quantification of diameter reduction due to corrosion in reinforcing steel bars, Structural Health Monitoring 14, 532–43, 2015.

[6] Wang, D., Ye, L., Su, Z., Lu, Y., Quantitative identification of multiple damage in laminated composite beams using A0 Lamb mode, Journal of Composite Materials 45 2061–9, 2011.

[7] Ihn, J B., Chang, F. K., Pitch-catch active sensing methods in structural health monitoring for aircraft structures, Struct. Health Monit., vol. 7, no. 1, pp. 5–19, 2008.

[8] Giurgiutiu, V, Structural Health Monitoring with Piezoelectric Wafer Active Sensors, 2nd Edition, Elsevier Academic Press, 1032 pages, ISBN 9780124186910, 2014.

[9] Pham, D. T., , Pham, P. T. N., Artificial intelligence in engineering, International Journal of Machine Tools and Manufacture, Volume 39, Issue 6, 1999.

[10] De Fenza, A., Sorrentino, A., Vitiello, P., Application of Artificial Neural Networks and Probability Ellipse methods for damage detection using Lamb waves, Composite Structures, vol 133, 2015.

[11] Dworakowski, Z., Ambrozinski, L., Packo, P., Dragan, K., Stepinski, T., Application of artificial neural networks for compounding multiple damage indices in Lamb-wavebased damage detection, Structural Control and Health Monitoring 22 50–6, 2015

[12] Paixão, J. A. S., Hotspot Monitoring of Delamination Area in Composite Structures Using Gaussian Process Regression Model, Unpublished phD thesis. UNESP – Ilha Solteira, 2020.

[13] Lee, J.-S.; Park, G.; Kim, C.-G.; Farrar, C. R. Use of relative baseline features of guided waves for in situ structural health monitoring. Journal of Intelligent Material Systems and Structures, 2011.

[14] Gresil, M., Giurgiutiu, V., Shen, Y., Poddar, B., Guidelines for Using the Finite Element Method for Modeling Guided Lamb Wave Propagation in SHM Processes, 6th European Workshop on Structural Health Monitoring, 2012

[15] G. Papazafeiropoulos, M. Muñiz-Calvente, E. Martinez-Pañeda. Abaqus2Matlab: A suitable tool for finite element post-processing. Advances in Engineering Software. Vol 105. March 2017.